<div align="center">

Supporting information for

</div>

Glass-phase coordination polymer displaying proton conductivity and guest-accessible porosity

Munehiro Inukai, Yusuke Nishiyama, Kayako Honjo, Chinmoy Das, Susumu Kitagawa, and Satoshi Horike

Contents

Fig. S10. 2D ^{1}H-^{1}H DQNMR spectrum of **1g**

S9. Single crystal X-ray diffraction

Table S1. Crystallographic data for **1**

S1. Syntheses

Syntheses of [{Zn$_2$(HPO$_4$)$_2$(H$_2$PO$_4$)}(ClbimH$^+$)$_2$·(H$_2$PO$_4^-$)·(MeOH)]$_n$ (1), activated 1 (1a), and glass-form 1 (1g)

All chemicals employed were obtained from commercial suppliers and used without further purification. ZnO (81 mg, 1 mmol), 5-Chloro-1H-benzimidazole (153 mg, 1 mmol), phosphoric acid (85% solution, 205 μl, 3 mmol) and MeOH (200 μl) were stirred in a mortar until the mixture become paste. The obtained red paste was washed with MeOH three times to get dry pure-phase. **1** was heated at 120°C under vacuum for 6 hours to obtain activated **1a**. Glass-form **1** was prepared by melt-quenching. **1a** was put in an oven preheated at 150 °C and stayed for 30 min. The molten **1a** was cooled in air at room temperature to obtain **1g**. ZnO (81 mg, 1 mmol), 5-Chloro-1H-benzimidazole (153 mg, 2 mmol), phosphoric acid (85% solution, 205 μl, 3 mmol) and MeOH (200 μl) were stirred in a vial and let the reagents react at room temperature for 6 h to obtain single crystals.

S2. Physical measurements

X-ray powder diffraction (XRPD) patterns were collected on a Rigaku SmartLab and Rigaku MiniFlex II with CuKα radiation. Thermogravimetry analysis (TGA) in the temperature range of 303-773 K was performed using a Rigaku Thermo plus EVO2 under flowing nitrogen with 20 K min^{-1} ramp rate. The adsorption and desorption of water and methanol 298 K were measured by a BELSORP-aqua instrument. ^{1}H-^{31}P MAS and ^{1}H-^{31}P cross polarization MAS (CP-MAS) NMR spectra of **1** and **1a** were recorded on a Bruker ADVANCE 400 MHz spectrometer. Static magnetic field and MAS frequency were 9.4 T and 10 kHz. The signals were acquired under two-pulse phase modulating (TPPM) proton decoupling. The recycle delay and contact time were 15 s and 2 ms. All MAS NMR of **1g** were performed on a JNM-ECA600. Static magnetic field and MAS frequency were 14.1 T and 70 kHz. The recycle delay and contact time were 20s and 2 ms. Two-dimensional ^{1}H-^{1}H double-quantum filter (2D ^{1}H-^{1}H DQNMR) spectra were obtained with back-to-back (BaBa) pulse sequence. To assign peaks in the ^{1}H MAS spectra, ^{1}H-^{14}N multiple Quantum Coherence (HMQC) and ^{1}H-^{31}P double cross polarization (double CP) spectra were carried out. WALTZ-16 was used as decoupling pulse sequence. The contact time for double CP was 3 ms. Single crystal X-ray diffraction data at 223 K were collected using a Rigaku X-ray diffractorometer with a confocal monochromated MoKα radiation. The deposited number of Cambridge Crystallographic Data Centre (CCDC) is 1907325.
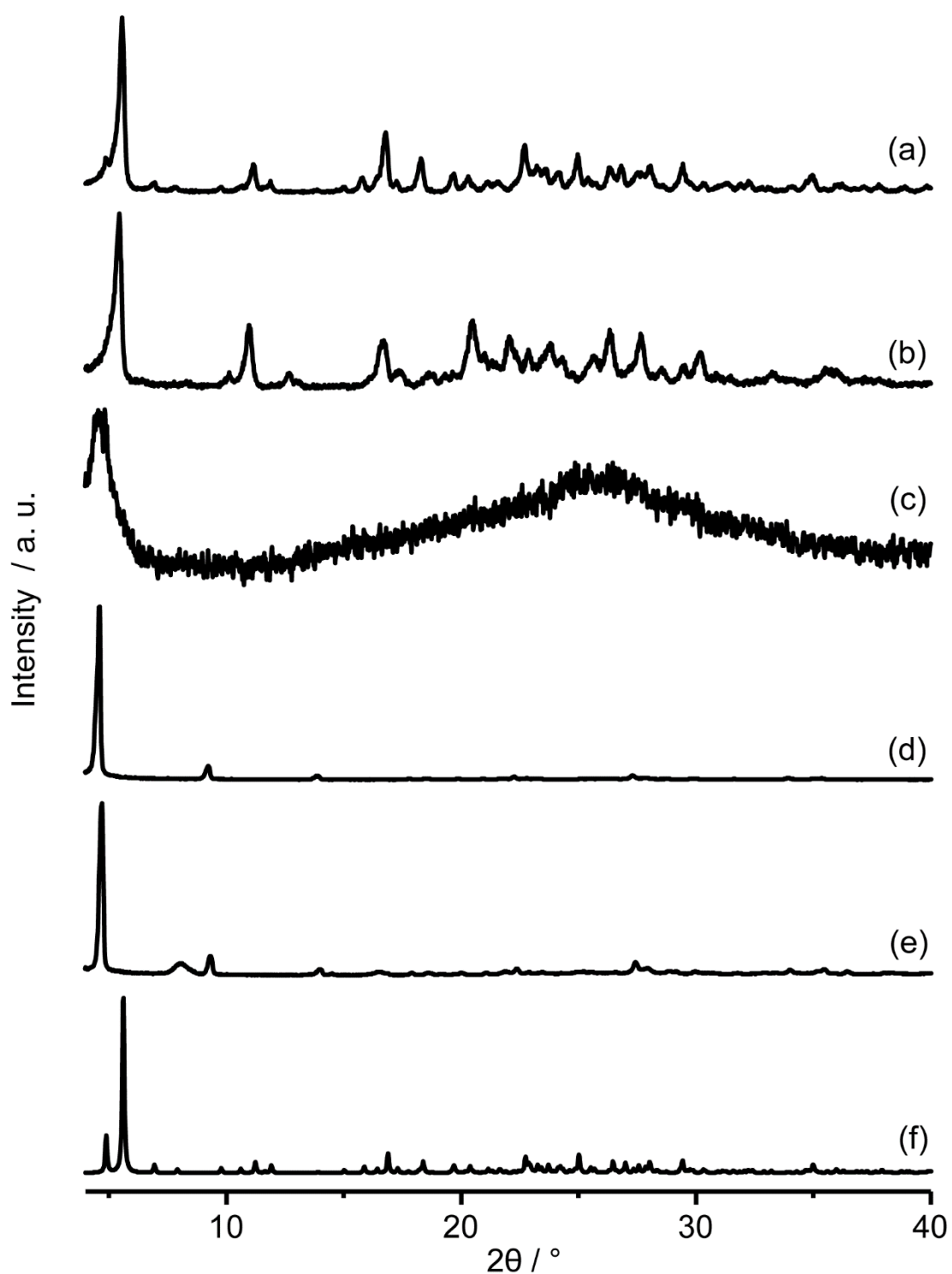
S3. Powder X-ray diffraction patterns (PXRD)

Fig. S1. PXRD patterns of (a) **1**, (b) **1a**, (c) **1g**, (d) **1a** after heating at 80 °C under 95 % relative humidity, (e) **1g** after heating at 80 °C under 95 % relative humidity, and (f) calculation from crystal structure of **1**. The PXRD patterns after the heating under the humid condition display large differences compared to those of original CPs, suggesting structural transition to another crystal structure.
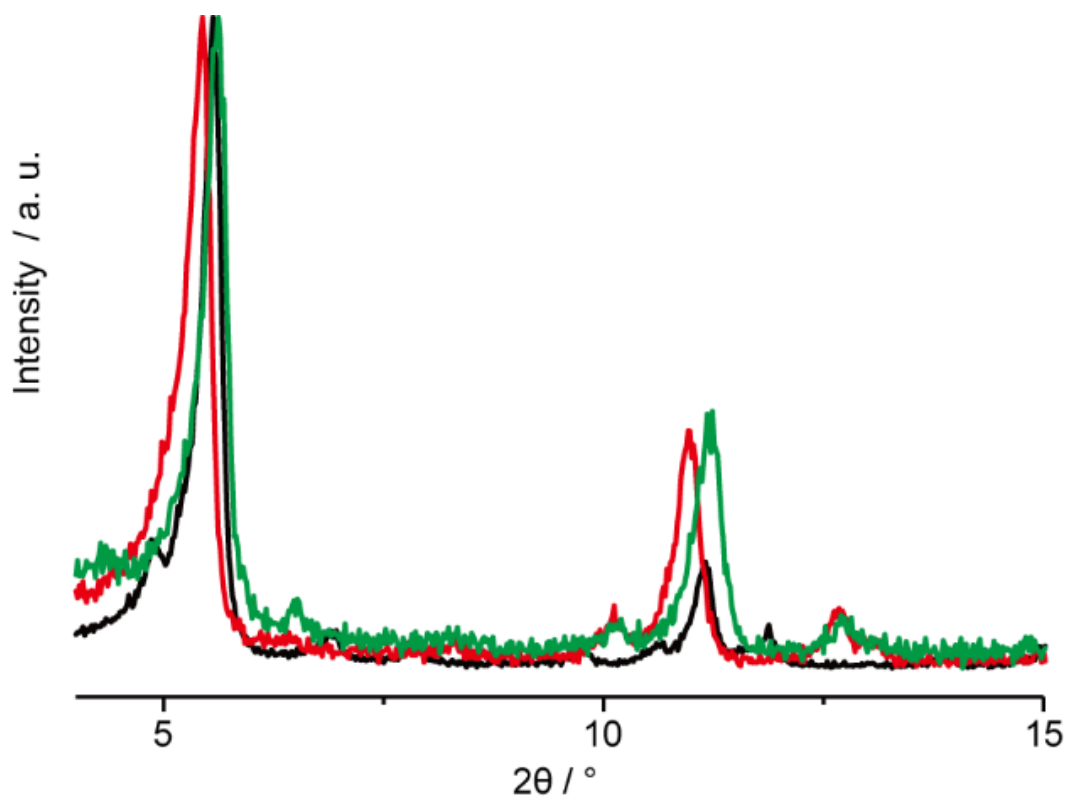
Fig. S2 PXRD patterns of **1** (black), **1a** (red), and **1a** after adsorption of MeOH (green) in the range of 4-15°. After the removal of MeOH, some peaks related 2-D frameworks (e.g. 5.5° and 11.2° indicating [010] and [020]) are slightly shifted, indicating shrinkage of the distance between 2-D frameworks. After adsorption of MeOH in **1a**, the peaks back to the original positions. This indicates that the layer distance expands and backs to the original on during the adsorption of MeOH.

S4. Thermogravimetric analysis (TGA) and differential scanning calorimetry (DSC)
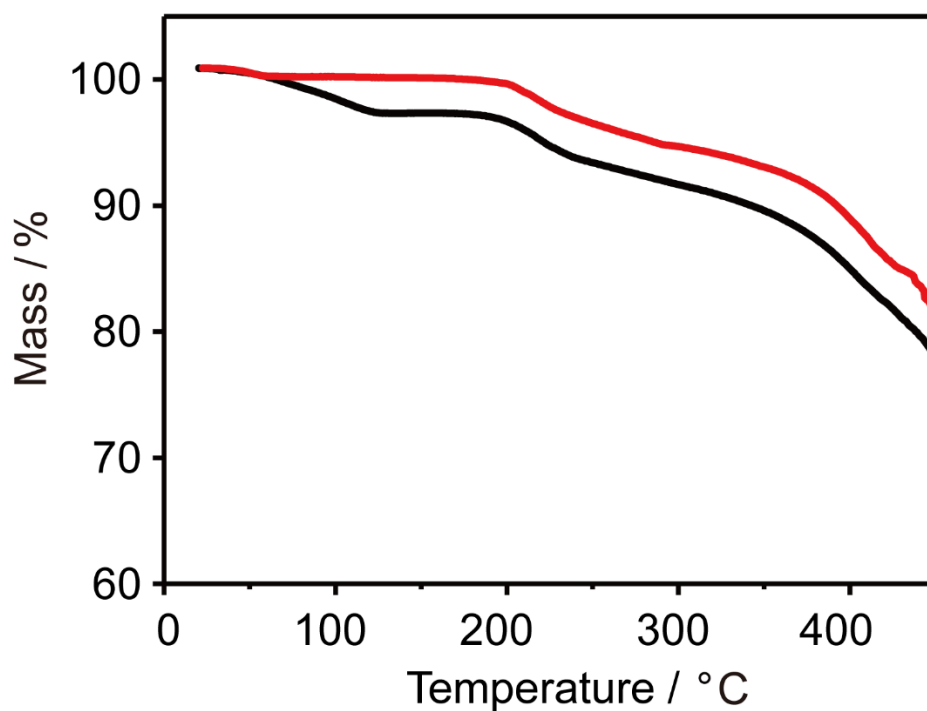

Fig. S3. TGA profiles of **1** (black) and **1a** (red). The weight loss in the profile of **1a** at 130°C is 3.6%, which is well corresponding to that of MeOH (calculated weight loss 3.6 %).
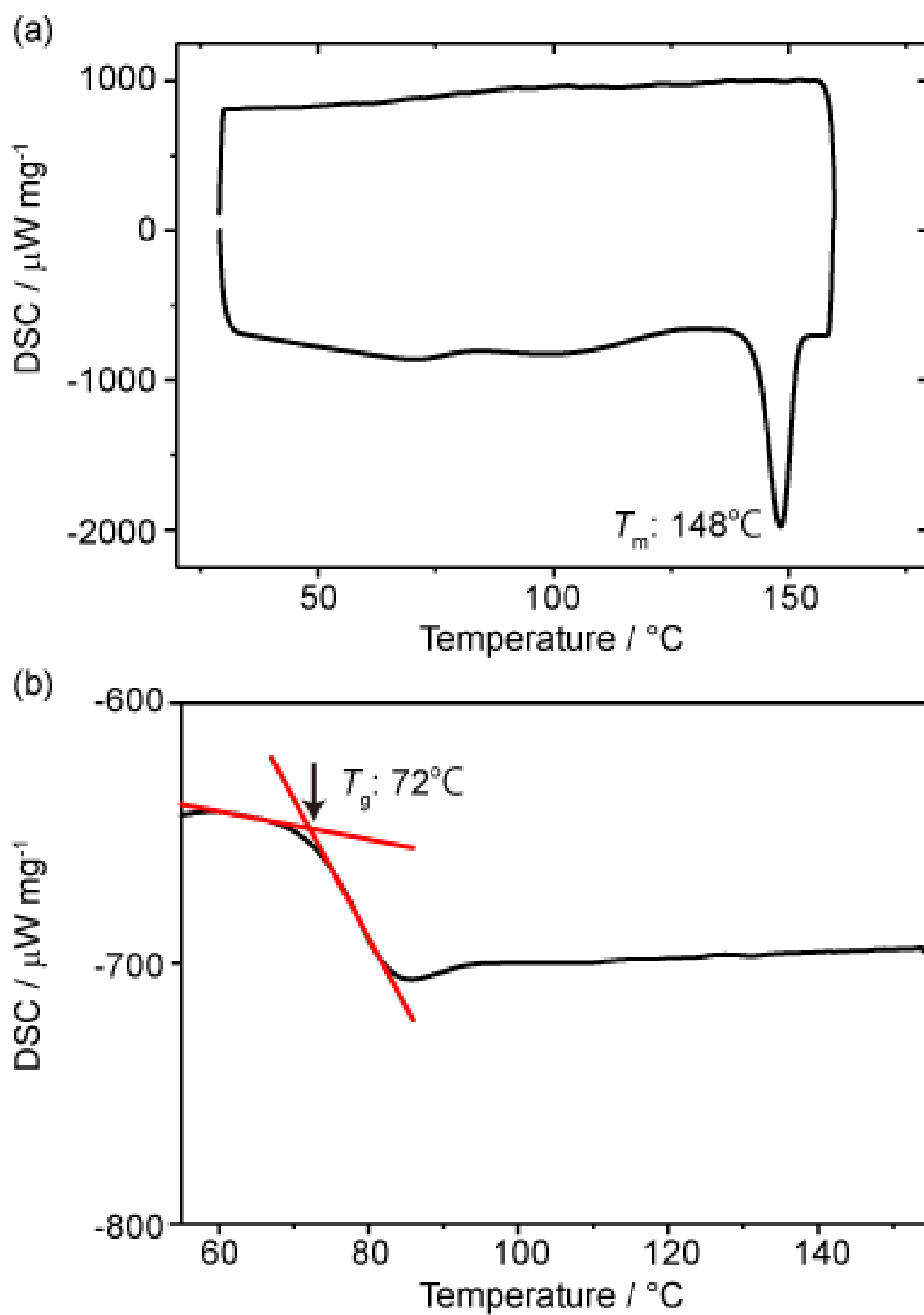
Fig. S4. DSC curves of (a) **1a** and (b) **1g**.
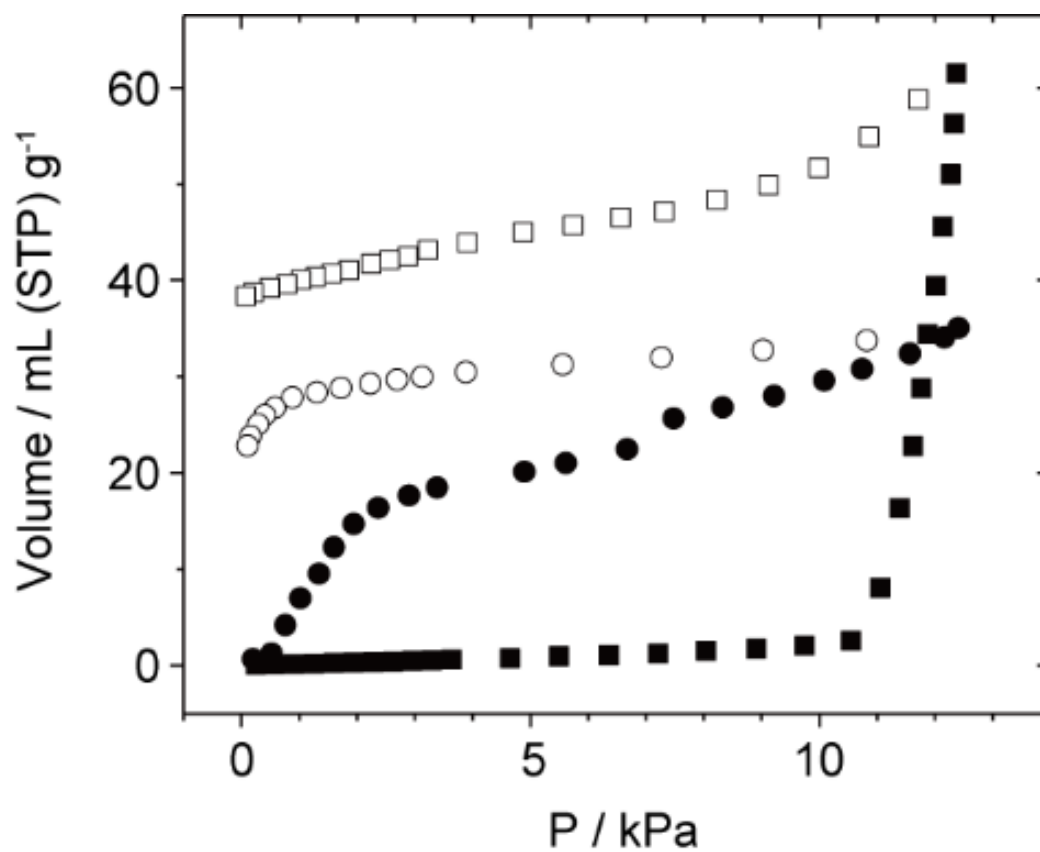
S5. Adsorption isotherms

Fig. S5. Adsorption isotherms of methanol at 298 K for **1a** (circle) and **1g** (square). Closed and open circles represent adsorption and desorption, respectively.
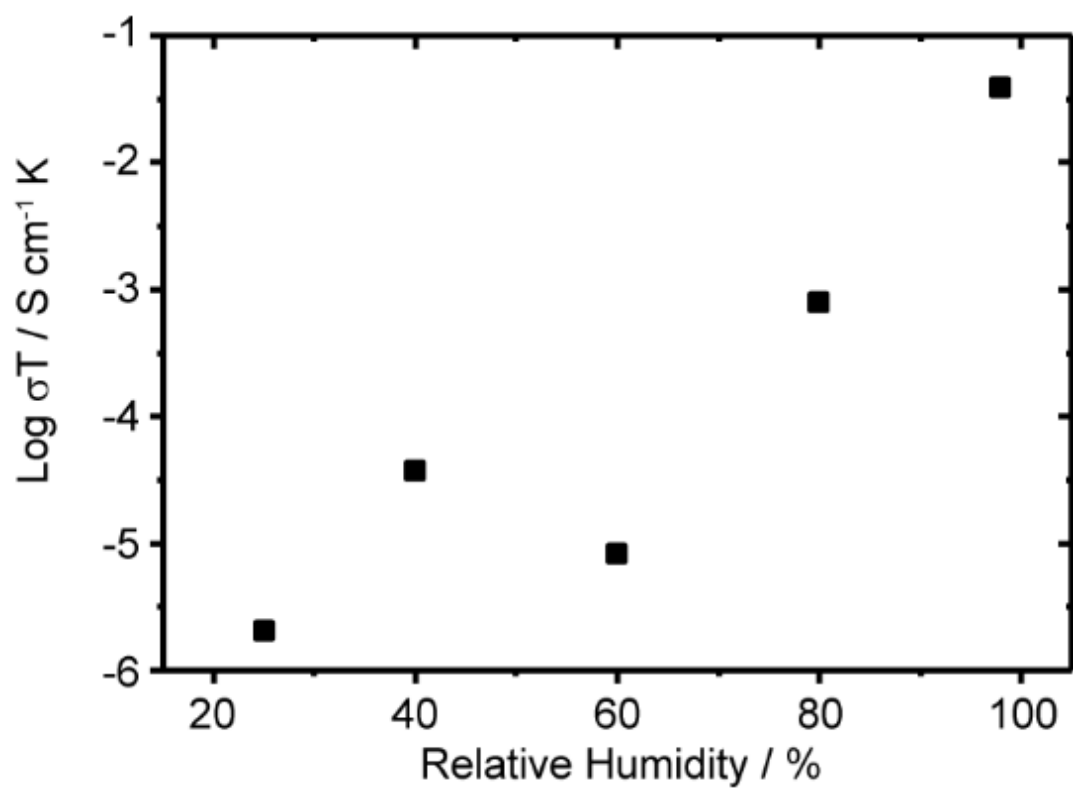
S6. AC impedance measurement

Fig. S6. Proton conductivity of **1g** under various humidity conditions at 298 K.

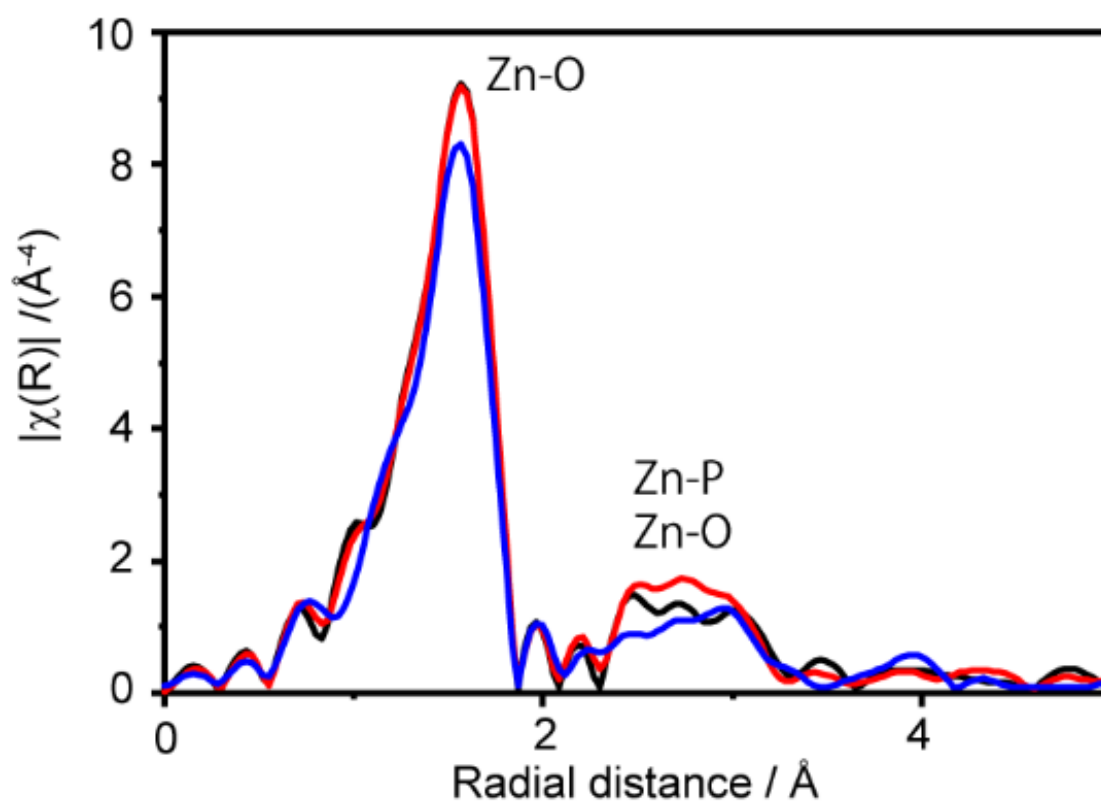# S7. Extended X-ray absorption fine structure analyses (EXAFS)

Fig. S7. RDFs from Zn K-edge EXAFS spectra of **1** (black), **1a** (red), and **1g** (blue) at room temperature.
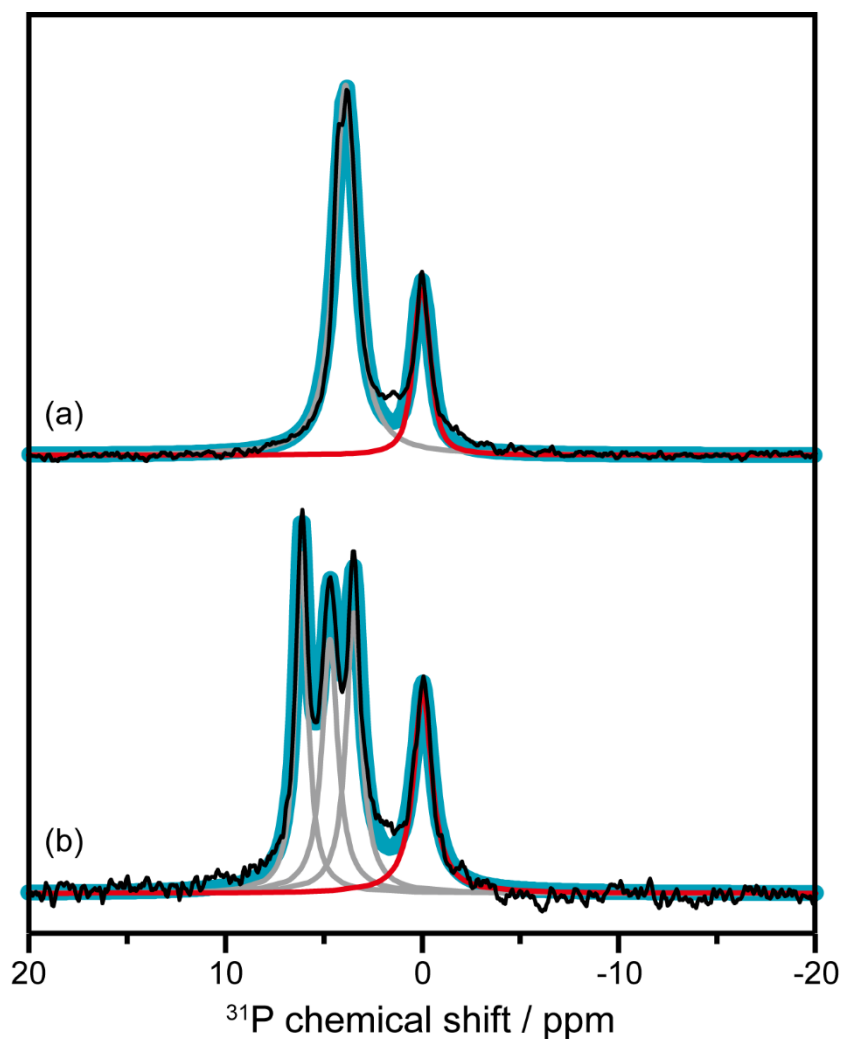
S8. Solid-state NMR analyses

Fig. S8. ^{31}P MAS NMR of (a) **1a** and **1g** at room temperature. Black and blue lines correspond to the experimental and fitted spectra, respectively. The fitted spectra are composed of the spectra of the uncoordinated phosphate (red) and the coordinated phosphates (gray). The ratio of peak intensities between uncoordinated phosphates and coordinated phosphates is 24:76 (**1a**) and 23:77 (**1g**), respectively. The ratios are approximately equal to the stoichiometric ratio of **1a** (25:75), suggesting that uncoordinated phosphates are tightly encapsulated as well as the crystal structure of **1**.
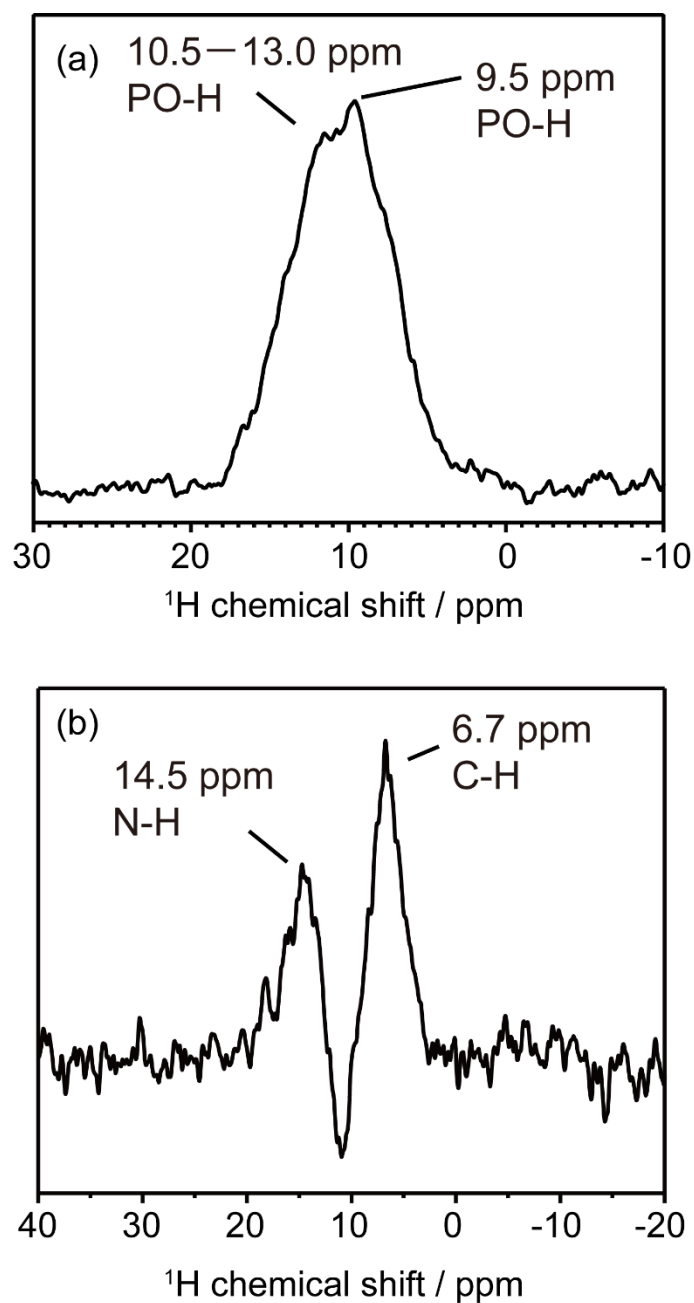
Fig. S9. (a) 1D ^{1}H–^{31}P double CP-MAS and (b) 1D ^{1}H–^{14}N hetero-nuclear multiple quantum coherence (HMQC) spectrum of **1g**. The ^{1}H–^{31}P double CP-MAS and ^{1}H–^{14}N HMQC spectrum includes peaks at 9.5 and 10.5–13.0 ppm assigned to the O–H moiety of the phosphate ions within the 2D frameworks and a peak at 14.5 ppm assigned to the N–H moiety of Clbim. Other large peaks in the spectrum can are assigned to the C–H moiety of Clbim.
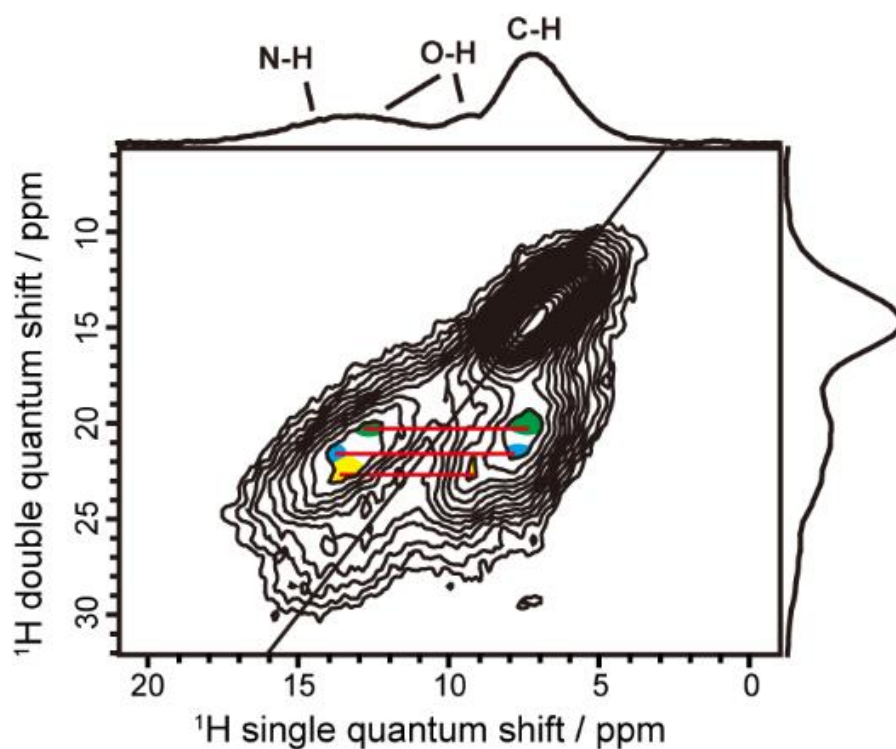
Fig. S10. 2D ^{1}H-^{1}H DQNMR spectrum of **1g** at room temperature. The red lines connect the correlation peaks between O–H and C–H (green), N–H and C–H (blue), and N–H and O–H (yellow). The 2D ^{1}H–^{1}H DQNMR spectrum of **1g** is characterized by the presence of three peaks pointing to a correlation between Clbim (N–H and C–H) and the 2D frameworks (O–H). These correlations reflect the homogenous distribution of Clbim molecules in the 2D frameworks.

S9. Single crystal X-ray diffraction

Table S1. Crystallographic data for **1**.

Compound	**1**
Temperature	223 K
Space Group	Triclinic P-1
a / Å	5.159(3)
b / Å	15.964(8)
c / Å	18.237(10)
α / °	97.386(10)
β / °	91.735(8)
γ / °	96.000(12)
Volume / Å^3	1479.8
Z	2
R	0.0865
wR_2	0.2031
GOF	1.058